〈Technical Note〉

SHIELDED LASER ABLATION ICP-MS SYSTEM FOR THE CHARACTERIZATION OF HIGH BURNUP FUEL

YEONG-KEONG HA*, SUN HO HAN, HYUN GYUM KIM, WON HO KIM and KWANG YONG JEE
Korea Atomic Energy Research Institute,
1045 Daedeokdaero, Yuseong-gu, Daejeon 305-353, Korea
*Corresponding author. E-mail : nykha@kaeri.re.k

Received December 26, 2007
Accepted for Publication March 6, 2008

In modern power reactors, nuclear fuels have recently reached 55,000 MWd/MtU from the initial average burnup of 35,000 MWd/MtU to reduce the fuel cycle cost and waste volume. At such high burnups, a fuel pellet produces fission products proportional to the burnup and creates a typical high burnup structure around the periphery region of the pellet, producing the so called 'rim effect'. This rim region of a highly burnt fuel is known to be ca. 200 μm in width and is known to affect the fuel integrity. To characterize the local burnup in the rim region, solid sampling in the micro meter region by laser ablation is needed so that the distribution of isotopes can be determined by ICP-MS. For this procedure, special radiation shielding is required for personnel safety. In this study, we installed a radiation shielded laser ablation ICP-MS system, and a performance test of the developed system was conducted to evaluate the safe operation of instruments.

KEYWORDS : Shielded Laser Ablation ICP-MS, Micro Sampling, High Burnup Fuel

1. INTRODUCTION

In the modern nuclear industry, a great endeavor has been made to reduce the fuel cycle cost and waste volume by increasing the burnup of a nuclear fuel. For this end, the fuels used in PWR reactors have recently reached 55,000 MWd/MtU from the initial average burnup of 35,000 MWd/MtU, and a significant increase of up to 100,000 MWd/MtU is expected in the coming years [1]. A nuclear fuel produces fission products proportional to the burnup and creates a highly porous and fine grain size micro structure at the pellet periphery by a higher fission gas release at high burnup [2]. Among the burnup dependant properties, the radial distribution of fission products in spent fuel is our main concern to verify the local burnup of highly burnt fuel.

In general, the analysis of fission products is carried out by an inductively coupled plasma mass spectrometer (ICP-MS) after dissolution of a fuel pellet. However, when analyzing the radial distribution of the fission products from the core to the rim of a spent fuel pellet, methods based on the dissolution technique are inadequate [3,4]. Currently, electron-probe micro analysis (EPMA)[5] and secondary ion mass spectrometry (SIMS)[6,7] are used to analyze the spatial distribution of fission products from highly radioactive solid samples. EPMA has the advantage of a high spatial resolution, but it does not give isotopic information. SIMS has the advantages of high sensitivity and accurate isotopic measurements with excellent spatial resolution; however, it is quite expensive.

For the direct analysis of a solid sample without any chemical pretreatment, a laser ablation (LA) was chosen as a sampling method for ICP-MS. This method can be used to analyze the spatial distribution of elements in a solid sample by micro sampling with a laser beam. Thus, for the direct analysis of the isotopes and their radial distribution in a spent fuel, we developed a radiation shielded laser ablation ICP-MS system [8-10]. The performance of this system was tested, and an analysis of the isotopic ratio in a simulated nuclear fuel (SIMFUEL) was carried out. The goal for this radiation shielded LA-ICP-MS system was to achieve less than 50 μm spatial resolution with less than ±10% standard deviation.

2. FABRICATION OF A SHIELDED LASER ABLATION SYSTEM

2.1 Laser Ablation System

As an adequate commercial LA system was not available for the analysis of a highly radioactive material, we have developed a laser ablation system in conjunction with ICP-MS, for the direct analysis of the fission products and their radial distribution in a spent fuel. The LA

system was designed as shown in Fig. 1. It consists of a laser source, image analyzer, XYZ translator with motion controller, ablation chamber, and various optics. As a laser source, a Q-switched Nd:YAG laser (SLMQ1S-20, Spectron Laser Systems) was used at the primary wavelength of 1064 nm with optical components to quadruple (266 nm) the frequency. The laser can be operated with a pulse repetition rate from 1 to 20 Hz, and maximum pulse energy of 4 mJ. The laser beam should have Gaussian shape with the "flat-top" mode, which creates uniform and reproducible craters [11]. For a homogeneous and flat-top-shaped beam profile, Tem_{00} mode was used. The laser beam was guided onto the sample surface by 90° reflection mirrors and a focusing lens (focal length 60 mm).

There are different types of ablation chambers

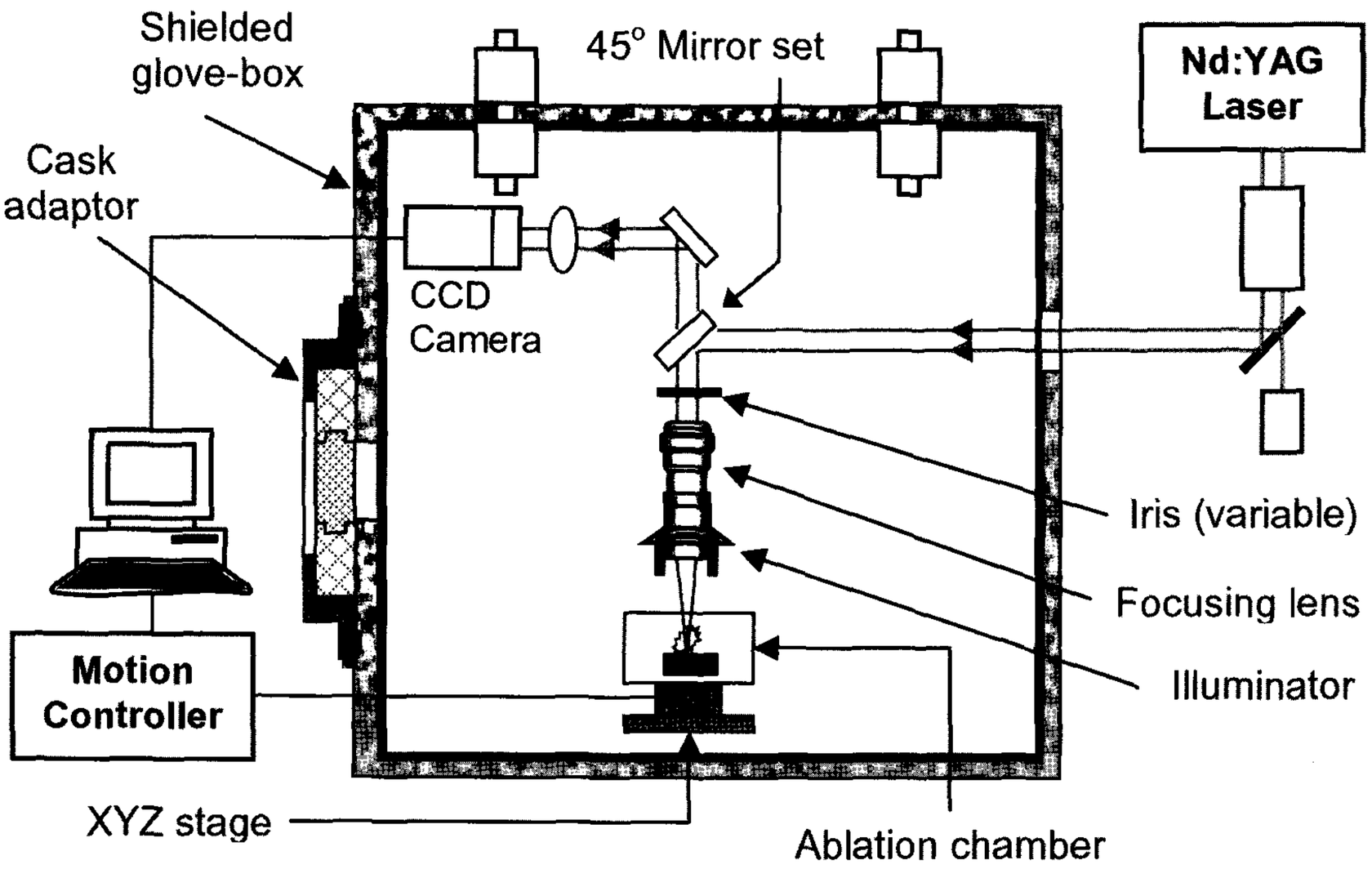

Fig. 1. Layout of Radiation Shielded Laser Ablation System

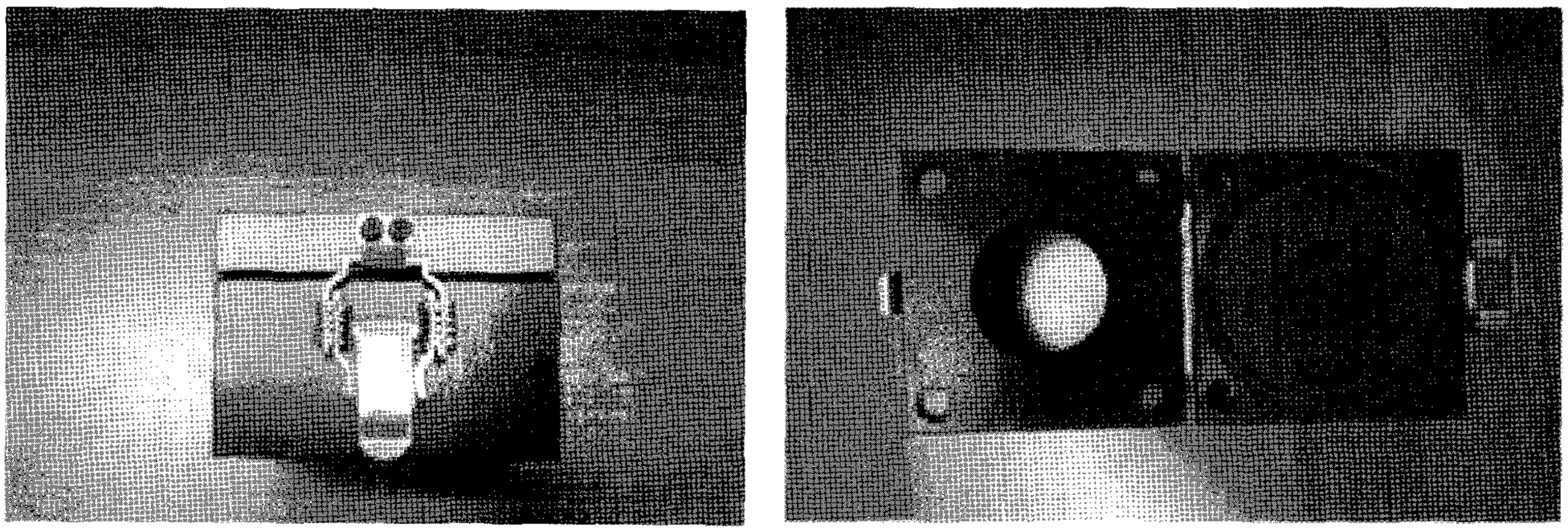

(a) front view (b) top view

Fig. 2. Ablation Chamber for the Shielded LA System

designed by many researchers [12,13]. For a highly radioactive material, as the ablation chamber has to be handled easily by manipulators, a hinge and a clip was attached to the lid for easy opening and closing, and a replaceable fused silica window was installed for transmission of UV laser light. Regarding the dimensions of the specimen mold, the main body has a sample hole of 30 mm (diameter) x 20 mm (depth) as a sample platform. It also has open wings across the sample hole of 10 mm in depth for a manipulator to grab a sample easily. Both sides of the sample hole have slits for the transportation of ablated particles to the ICP-MS (Element, Finnigan) via argon carrier gas. Figure 2 shows the ablation chamber designed by this group. Right under the ablation chamber, a three-dimensional linear translator (XYZ stage) was installed with a motion controller (LabMotion series-640 smartstage and stepper drive module SDM-1, COHERENT) for a precise and accurate movement. The travel distance of the translator is 50 mm with a minimum movement of 1μm.

To adjust the sampling position and to observe the spot size and its shape, an imaging device composed of a CCD camera (CV-S3200, JAI), a TV tube (OPTEM), an object lens, and an illuminator was installed. The magnification of the viewing optics is x500.

2.2 Radiation Shielded Glove Box

To analyze highly radioactive materials, radiation shielding is required to protect personnel. The shielded glove box was designed so that the maximum dose received by the operator is lower than 25 μSv/h. Shielding calculation was performed conservatively by QAD-CG, assuming the maximum radioactivity of a sample specimen is 1 Ci based on the estimated radioactivity of a spent fuel pellet (50,000 MWd/MtU, 3 years cooling, 0.3 g), which corresponds to ca. 0.3 Ci. Lead was used as the shielding material with a wall thickness of 70 mm. A shielding model for the glove box is shown in Fig. 3, and the calculated dose rates at each side of the glove box are listed in Table 1.

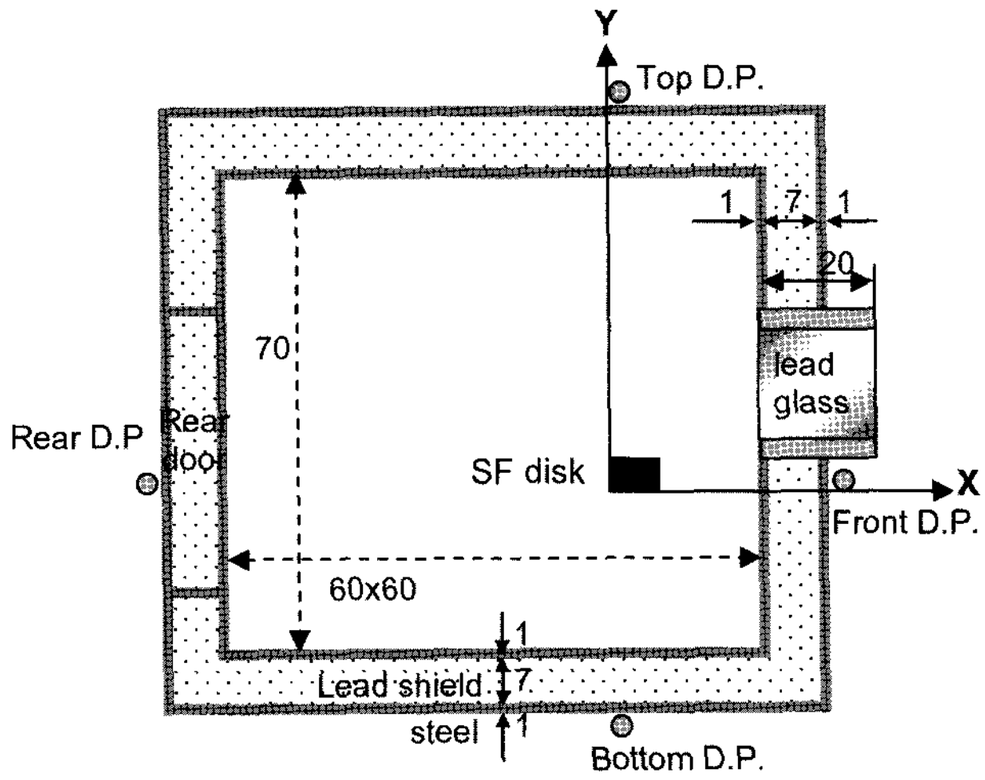

Fig. 3. Shielding Model for Glove Box and dose Rate Detection Points

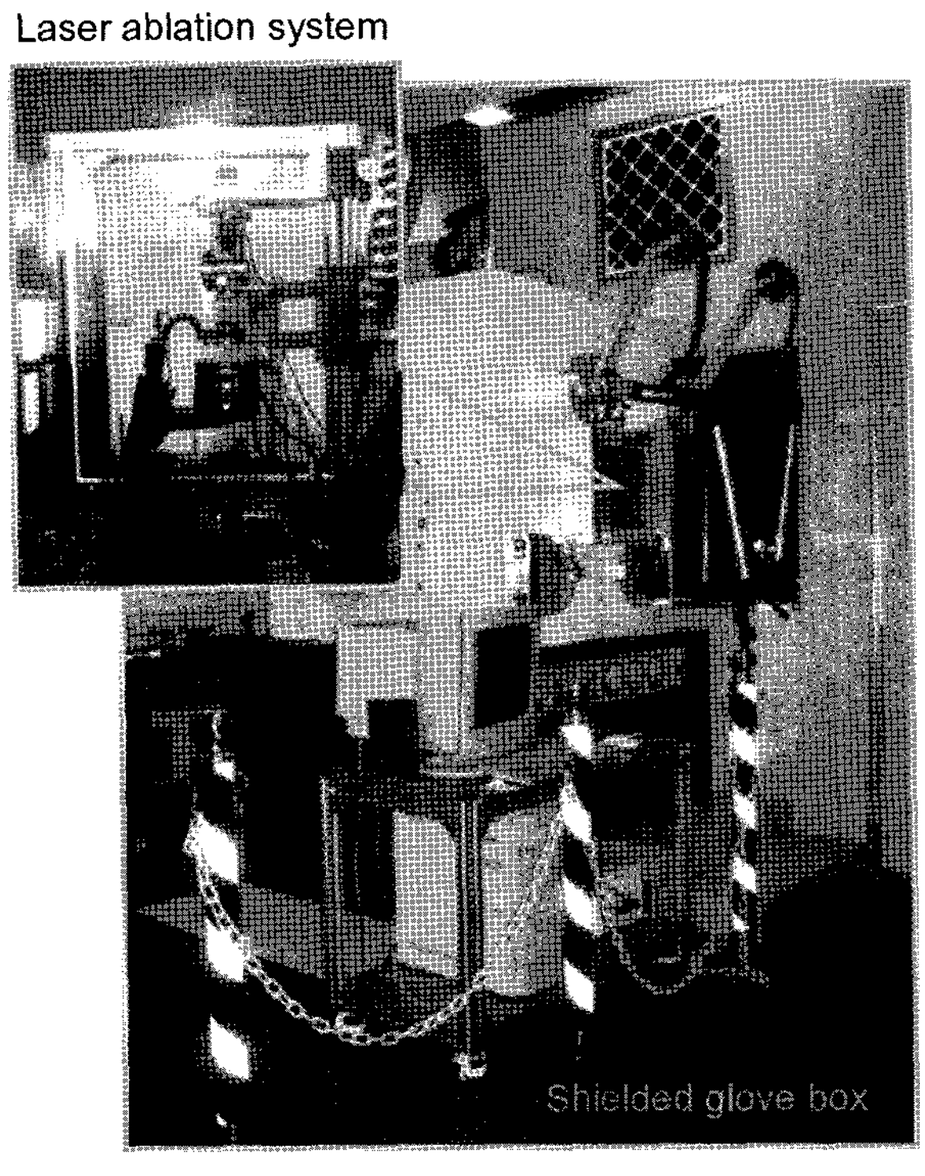

Fig. 4. Radiation Shielded Laser Ablation System

Table 1. Dose rates Calculated by QAD-CG for 1 Ci Sample at the Surface of the Glove Box Shielding Wall

Detection point	Dose rate	Remark
Front wall surface (D.P 1)	12 μSv/hr	
Bottom wall surface (D.P 2)	11 μSv/hr	Allowable limit:
Top wall surface (D.P 3)	4.6 μSv/hr	25 μSv/hr
Side wall surface (D.P 4)	5.0 μSv/hr	
Rear door surface (D.P 5)	9.9 μSv/hr	

Details of the glove box design, shown in Fig. 4, are as follows. Each wall was cast in 70 mm thick lead between two stainless steel plates of 10 mm thickness. The front panel consisted of a lead glass window, two mini manipulators (R.W. Wiesener, Inc.), and a pair of glove

ports. The rear panel has a maintenance door and a fused silica window for the UV laser entrance. The floor panel has three utility line holes for the XYZ-translators, the carrier gas, and the imaging device. The roof panel has a lighting system and inlet/outlet filter boxes for ventilation. The outlet filter box was connected to the negative pressure line to maintain a negative pressure inside the glove box. The left side panel has a cask adapter and a specimen entrance hole. The cask adapter on the glove box fits securely with the specimen transportation cask.

The CCD camera, XYZ translator, ablation chamber, and various optics were installed inside the glove box, while the Q-switched Nd:YAG laser, optics, motion controller, and associated electronics were located outside. To operate the system efficiently, a mini manipulator was equipped on the front panel of the shielded glove box. The laser beam was transferred into the glove box via two 90° UV mirrors and a UV window on the maintenance door. The laser ablation system was coupled to the ICP-MS (Element, Finnigan) using a PVC tube with an argon flow of 1 l/min.

3. PERFORMANCE TEST OF RADIATION SHIELDED LA-ICP-MS SYSTEM

3.1 Spatial Resolution of Shielded Laser Ablation System

Characterization of the localized chemical properties from core to rim of a spent fuel was our main concern. The 'rim' region caused by high burnup is known to be ~200 μm wide. To observe the rim effect, more than 3~5 data points in the rim region are needed. Therefore, the goal for this radiation shielded LA-ICP-MS system was to achieve a spatial resolution of less than 50 μm. A zircaloy-4 (Zry-4) plate was used as a test specimen for the performance test of the developed system. The changes of the crater size with respect to the focusing distance at various laser pulse energies are shown in Fig. 5. The figure shows that the crater size decreased until the defocusing distance reached ca. 3,000-3,500 μm. This defocusing distance may result from the different focal length between the camera lens and the incident laser beam. Also shown in Fig. 5 is that a crater size of smaller than 50 μm was achieved when the laser power was below 50 %. From these results, we concluded that the target value of the spatial resolution (< 50 μm) can be achieved at a laser power below 55% with a 3,000-3,500 μm defocusing distance.

Figure 6 shows the ablated craters of Zry-4 within a 1 mm thickness at 10 Hz, at 55% laser power with a 3,500 μm defocusing distance. To examine the accuracy and precision of the movement, the translator was operated at 100 μm intervals, and the craters produced on the Zry-4 surface were observed by CCD camera. From the flat-bottomed, round shaped craters, we found that the power distribution of the laser beam is of sufficient homogeneity.

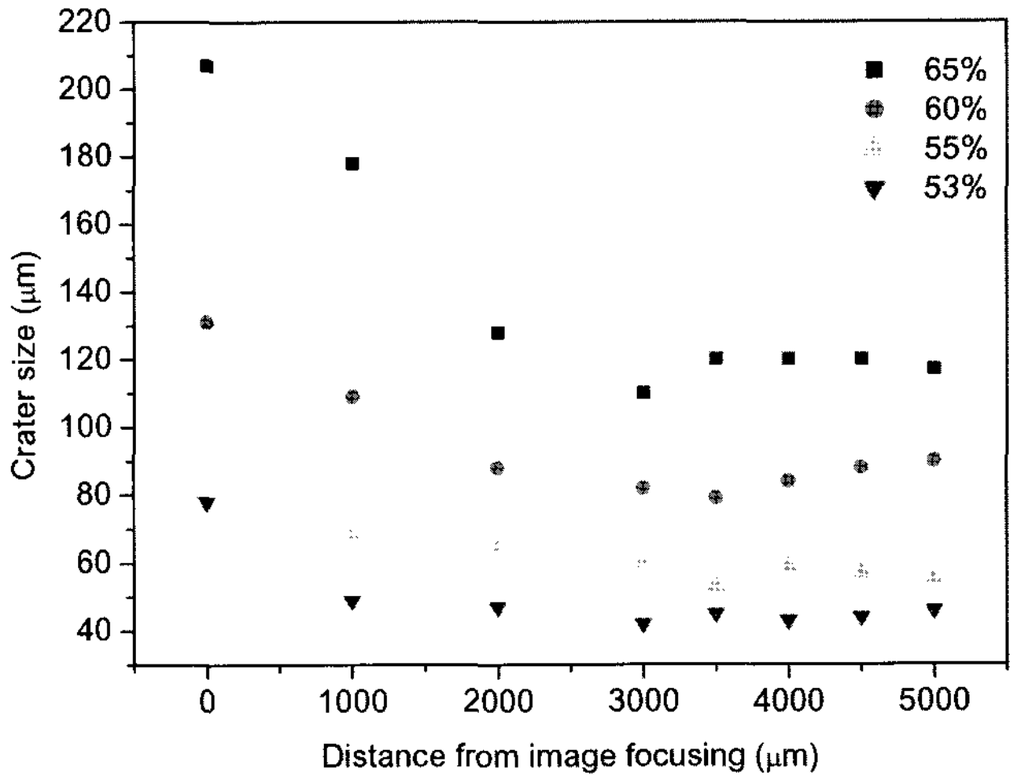

Fig. 5. Changes in Crater Size as a Function of Defocusing Distance at Various Laser Powers

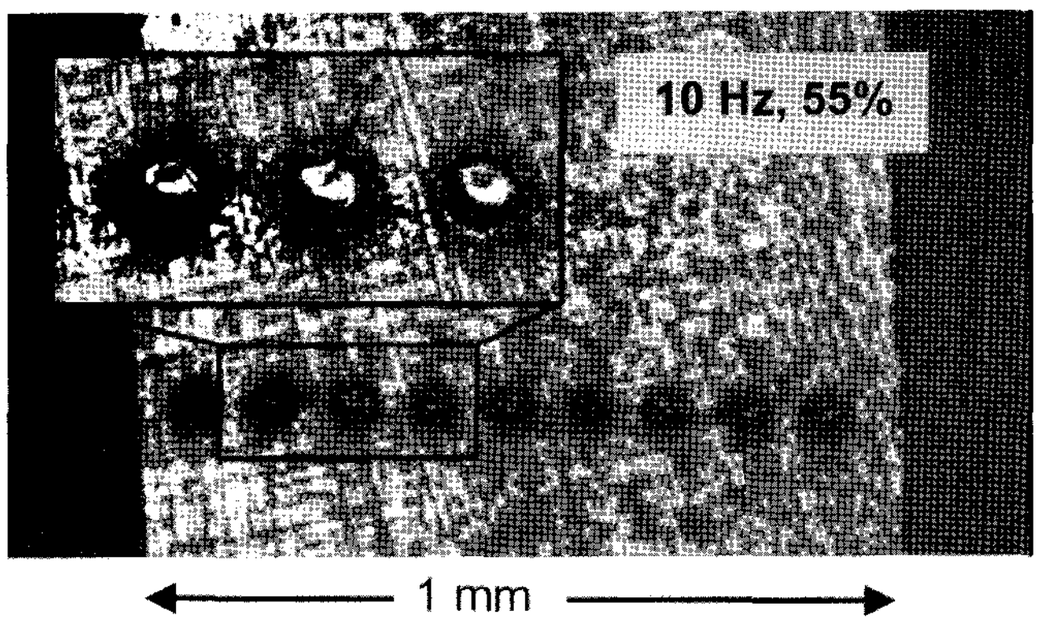

Fig. 6. Ablation Craters Formed on a Zry-4 Plate (Thickness: 1 mm) at 10 Hz, 55% Laser Power with 3500 μm Defocusing Distance

3.2 Precision

The NIST SRM 613 (61 elements in a glass matrix) was used as reference material to obtain the precision of the radiation shielded LA-ICP-MS system. Before the measurements, the ICP-MS system was optimized at maximum ion intensity for ^{238}U. Sampling was carried out using the laser beam from a Q-switched Nd:YAG laser at 266 nm. The laser was operated at 45 % laser power (4 mJ at 100%), 10Hz repetition rate and 2s sampling time. The ablated particles were transported to

Table 2. Operating Conditions of the ICP-MS System

Parameter		Conditions
ICP-MS	RF Power	1300 W
	Cooling gas flow	13 l/min
	Auxiliary gas flow	0.7 l/min
	Sampling gas flow	1.0 l/min
	Sample cone	Nickel with a 1.1 mm orifice
	Skimmer cone	Nickel with a 0.8 mm orifice
	Mass resolution	300 m/Δm
	Quadrupole working pressure	10^{-7}
	Detection mode	counting
Laser Ablation	Laser source	Nd:YAG 266 nm
	Laser power	45 % (4 mJ at 100 %)
	Repetition rate	10 Hz
	Sampling time	2 sec
	Beam profile	Tem_{00} mode

the plasma of the ICP-MS system through PVC tube. Measurement conditions of the ICP-MS system are summarized in Table 2.

Among the elements in the SRM 613, isotopic ratios of ^{139}La, ^{140}Ce, and ^{144}Nd against ^{238}U were measured. The concentrations of each element were 36, 39, and 36 ppm (values informed by the supplier rather than certified values) for La, Ce, and Nd and 37.38±0.08 ppm (certified value) for U, which corresponded to 0.259, 0.246, 0.059, and 0.156 μmole/g, respectively. The calculated atomic ratios regarding the isotopic abundance were 1.66, 1.57, and 0.38 for ^{139}La/^{238}U, ^{140}Ce/^{238}U, and ^{144}Nd/^{238}U, respectively. The isotopes in the SRM 613 were measured, and isotopic ratios against ^{238}U were calculated from the corresponding peak areas. As shown in Fig. 7, the measured values of the ratios were 0.95, 0.97, and 0.34 for ^{139}La/^{238}U, ^{140}Ce/^{238}U, and ^{144}Nd/^{238}U, respectively. The deviations between the measured and the calculated values may come from the difference in sensitivity of each element. The sensitivity factors calculated from the results were 1.75, 1.62, 1.12, and 1.0 for ^{139}La, ^{140}Ce, ^{144}Nd, and ^{238}U, respectively. The standard deviation of the four measurements were ±7 %, ±9 %, and ±5 % for ^{139}La/^{238}U, ^{140}Ce/^{238}U, and ^{144}Nd/^{238}U, respectively, which satisfied the target value for this system to achieve a precision of less than ±10%.

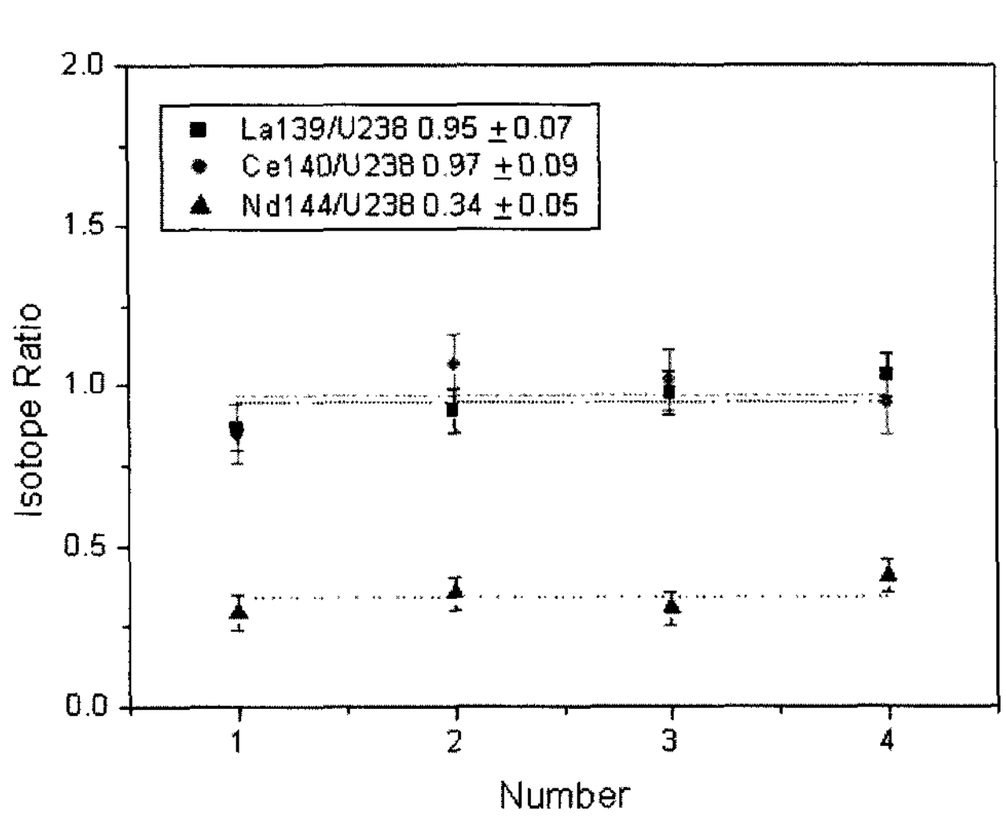

Fig. 7. Isotope Ratio of SRM613 Measured by the Shielded LA-ICP-MS System (Repetition rate: 10 Hz, Laser Power: 45 % (4 mJ at 100 %), Sampling Time: 2 s)

3.3 Distribution of ^{158}Gd in a Layered SIMFUEL

To measure the radial distribution profiles of isotopes in a spent nuclear fuel, a simulated fuel (SIMFUEL) was prepared. Among the fission product elements, Gd was chosen as a dopant because Gd is known to dissolve as a solid solution in UO_2 matrices [14,15] and to behave as a 'burnable poison'[6,7,16]. The Gd isotopes have a very high thermal neutron absorption cross-section of 61,000

and 254,000 barn for ^{155}Gd and ^{157}Gd, respectively. A few percent Gd addition to UO_2 prolongs the fuel life and maximizes the average fuel burnup.

A layered SIMFUEL specimen with nine different Gd compositions (y = 0~0.28) was prepared as follows.

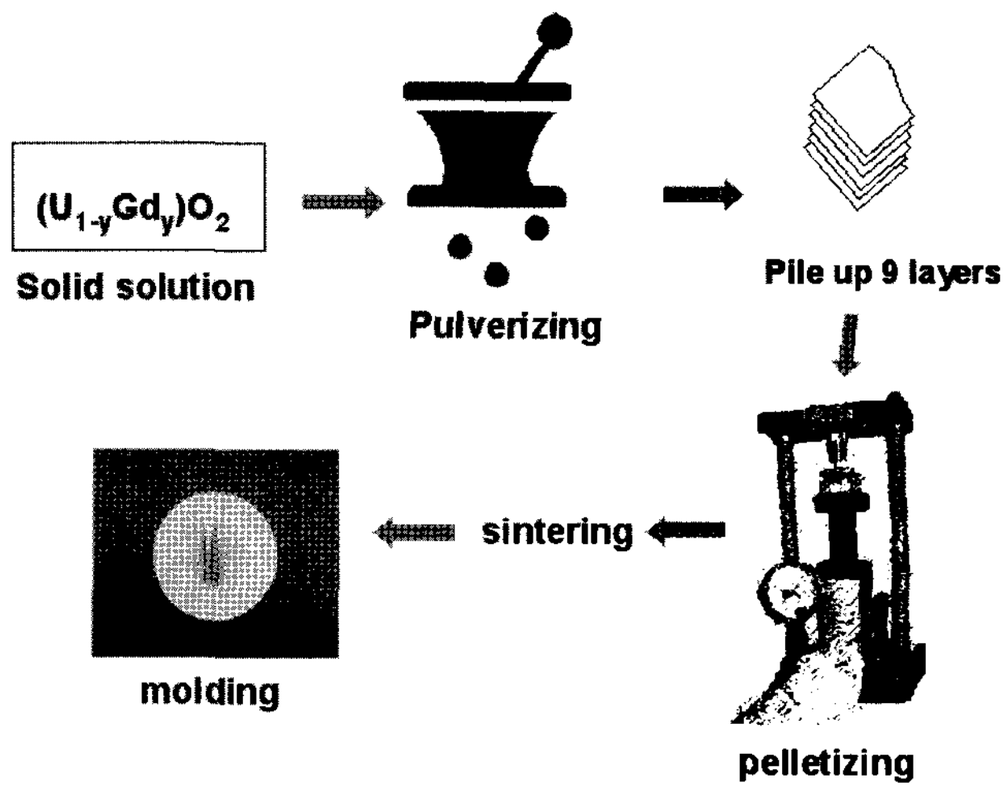

Fig. 8. Procedure for Preparing a Layered SIMFUEL Specimen

The powders of each layer, $(U_{1-y}Gd_y)O_2$ solid solution in the given range (y=0-0.28), were prepared from U_3O_8(U content was determined by potentiometric titration) and commercially available Gd_2O_3 (Aldrich, >99.999 %). Calculated amounts of U_3O_8 and Gd_2O_3 were mixed thoroughly by grinding in an agate mortar to a given composition of a solid solution $(U_{1-y}Gd_y)O_2$ where y ranged from 0 to 0.28. The powders were pelletized at 2 tons for 15 seconds then sintered at 1,700°C for 12 hours and annealed at 1,200°C for 12 hours under a hydrogen atmosphere. Each pellet was pulverized in an agate mortar. The prepared powders of $(U_{1-y}Gd_y)O_2$ solid solution were piled up in the order of y = 0, 0.023,0.045, 0.067, 0.088, 0.156, 0.277, 0.222, and 0.123 by compacting the powders layer by layer. The compacted powder was then pelletized at 2 tons for 10 seconds, and the pellet was sintered again under the same conditions described above. The specimen was sintered twice so that the compositions of each layer were analyzed individually and reactions between each layer at the boundary were minimized. The sintered pellet of layered SIMFUEL was embedded in epoxy resin and then polished. The dimensions of the prepared SIMFUEL were 2.4 (thickness) x 14 (length) x 3 (width) mm, with nine layers of uranium and gadolinium mixed oxide (Fig. 8). The nine layers had different Gd contents, and the composition of each layer and their calculated isotopic ratios are listed in Table 3.

The isotopic ratios of the layered SIMFUEL specimen were measured with the radiation shielded LA-ICP-MS. The experimental conditions were the same as described in 3.2. The sampling was performed along the layer at 300 μm intervals, so that eight points were measured for the spatial analysis. Figure 9 compares the calculated values of the $^{158}Gd/^{235}U$ ratio with the measured one. As shown in this figure, the measured $^{158}Gd/^{235}U$ ratios

Table 3. The Compositions of each Layer and the Calculated Isotopic Ratios

Layer	Composition, M(=U+Gd) in MO_{2-x}		Calculated isotopic ratio, $^{158}Gd/^{235}U$
	U (^{235}U), atomic %	Gd (^{158}Gd), atomic %	
0	100.0 (0.7)	-	-
1	97.7 (0.68)	2.3 (0.57)	0.84
2	95.5 (0.67)	4.5 (1.12)	1.67
3	93.3 (0.65)	6.7 (1.66)	2.55
4	91.2 (0.64)	8.8 (2.19)	3.42
5	84.4 (0.59)	15.6 (3.88)	6.58
6	72.3 (0.51)	27.7 (6.88)	13.49
7	77.8 (0.54)	22.2 (5.51)	10.20
8	87.7 (0.61)	12.3 (3.06)	5.01

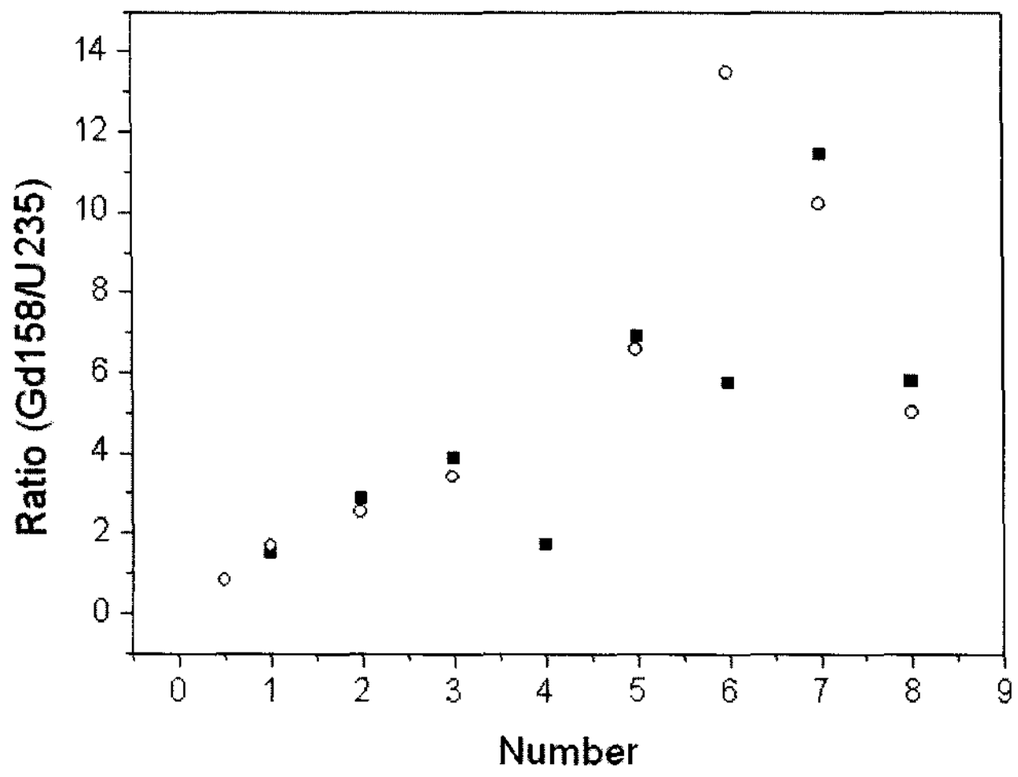

Fig. 9. Comparison Between Calculated and Measured Isotope Ratio, $^{158}Gd/^{235}U$ (○ : Calculated, ■ : Measured)

agreed comparatively well with the calculated values except for the 4th and 6th point. These two discrepancies were thought to be caused by contamination from neighboring layers during the powder packing process. It is known that the ablation efficiency is affected by heat conductivity, density, heat capacity, and vaporizing temperature of the material used, as well as the intensity of laser applied [11,17]. Therefore, sensitivity of the element depends on the elemental characteristics. However, the sensitivities (cps/atom) of Gd and U in the SIMFUEL obtained by this shielded LA-ICP-MS were almost equal (1:1). We concluded that the formation of a solid solution brings a very similar ablation tendency, because a Gd atom occupies a uranium site in the UO_2 lattice.

4. CONCLUSION

A radiation shielded laser ablation system was built for micro-sampling of radioactive solid specimens. Connecting with the ICP-MS system, this micro sampling system will be used for the analysis of the isotope distribution from core to rim of a spent nuclear fuel as well as irradiated fuels from a research reactor.

In the performance test, a spatial resolution of better than 50 μm was achieved at less than 55% laser power with 3,000-3,500 μm defocusing, which satisfies the target value for this system. Also, a precision of less than ±10% is acceptable for the spent fuel analysis. The measured values of elements forming solid solutions are quite reliable, although further studies are needed for the analysis of various fission products forming metallic precipitates, insoluble oxides, and volatile elements in a spent fuel. Thus, the shielded LA-ICP-MS constructed in this study can be applicable for producing the databases to interpret local burn up characteristics.

ACKNOWLEDGEMENTS

The authors thankfully acknowledge the financial support of the Nuclear Development Fund of the Ministry of Education, Science and Technology.

REFERENCES

[1] Z. Xu, M.S. Kazimi, M.J. Driscoll, "Impact of high burnup on PWR spent fuel characteristics", *Nuclear Science and Engineering*, **151**, p.261-273 (2005)

[2] Hi. Matzke, J. Spino, "Formation of the rim structure in high burnup fuel", *Journal of Nuclear Materials*, **248**, p.170 (1997)

[3] L. Neufeld and J. Roy, "Laser ablation solid sampling for plasma spectrochemistry", *Spectroscopy*, **19(1)**, p.16, (2004)

[4] R.E. Russo, X. Mao, H. Liu, J. Gonzalez and S.S. Mao, "Laser ablation in analytical chemistry-a review", *Talanta*, **57(3)**, p.425, (2002)

[5] C.T. Walker, "Electron probe microanalysis of irradiated nuclear fuel: an overview", *Journal of Analytical Atomic Spectrometry*, **14**, p. 447, (1999)

[6] H.U.Zwicky, T. Aerne, G, Bart, F. Petrik, H.A. Thomi, "Evaluation of the radial distribution of gadolinium isotopes in nuclear fuel pins by secondary ion mass spectrometry", *Radiochim. Acta*, **47**, p.9, (1989)

[7] S. Portier, S. Bremier, C.T. Walker, "Secondary ion mass spectrometry of irradiated nuclear fuel and cladding: An overview", *International Journal of Mass Spectrometry*, **263**, p.113, (2007)

[8] Y-K. Ha, S.H. Han, K.C. Han, K.Y. Jee, W.H. Kim, KRS:ISSN 1738-1142, **2(2)**, p.184, (2004)

[9] S.H. Han, Y-K. Ha, K.C. Han, Y.S. Park, K.Y. Jee, W.H. Kim, "Micro sampling system for highly radioactive specimen by laser ablation", *Journal of the Korean Radioactive Waste Society*, **3(1)**, p.17, (2005)

[10] Y-K. Ha, S.H. Han, Y.S. Park, S.D. Park, K.Y. Jee, W.H. Kim, KAERI/TR-3248/2006, (2006)

[11] J.C. Miller and R.F. Haglund, Jr., "Experimental methods in the Physical Sciences, **Vol. 30**; Laser Ablation and Desorption" Academic Press, (1998)

[12] P. Richner, M.W. Borer, K.R. Brushwyler and G.M.Hieftje, "comparison of different excitation sources and normalization techniques in laser ablation AES using a photodiode-based spectrometer", *Appl. Spectroscopy*, **44**, p.1290 (1990)

[13] M. Bi, A.M. Ruiz, I. Gornushkin, B.W. Smith and J.D. Winefordner, "Profiling of patterned metal layers by laser ablation inductively coupled plasma mass spectrometry", *Applied Surface Science*, **158**, p.197 (2000)

[14] H. Kleykamp, "The chemical state of fission products in oxide fuels at different stages of the nuclear fuel cycle", *Nuclear Technology*, **80**, p.412 (1988)

[15] J.G. Kim, Y-K. Ha, S.D. Park, K,Y. Jee, W.H. Kim, "Effect of trivalent dapant, Gd^{3+}, on the oxidation of uranium dioxide", *Journal of Nuclear Materials*, **297**, p.327 (2001)

[16] IAEA, International Atomic Energy Agency Report, "Characteristics and use of urania-gadolinia fuels", IAEA-TECDOC-844

[17] C.D. Allemand, "Spectroscopy of single-spike laser-generated plasmas", *Spectrochimica Acta*, **27B**, p.185 (1972)